T.C.
BOLU ABANT İZZET BAYSAL ÜNİVERSİTESİ
INSTITUTE OF GRADUATE STUDIES
DEPARTMENT OF CHEMISTRY

SYNTHESIS AND CHARACTERIZATION OF COBALT ORTHOBORATE NANOPOWDERS

MASTER OF SCIENCE, CHEMISTRY

SEDANUR DİMETOKALI

THESIS SUPERVISOR
Prof. Dr. Ayşe MORKAN
SECOND THESIS SUPERVISOR
Dr. Liska FADLIYANI

BOLU, 4/9/2025

ACCEPTANCE AND APPROVAL PAGE

The thesis entitled **SYNTHESIS AND CHARACTERIZATION OF COBALT ORTHOBORATE NANOPOWDERS** was presented and submitted by **Sedanur DİMETOKALI** in partial fulfillment of the requirements for the degree of **Master of Science** in Department of **CHEMISTRY** with majority vote is hereby approved. 4/9/2025

Jury Members	**Signature**
Supervisor Prof. Dr. Ayşe MORKAN Bolu Abant Izzet Baysal University	.....
Member Prof. Dr. Fazilet Devrim ÖZDEMİRHAN Bolu Abant Izzet Baysal University	.....
Member Prof. Dr. Mecit AKSU Düzce University	.....

Institute of Graduate Studies Approval

Prof. Dr. İbrahim KÜRTÜL

Director of Institute of Graduate Studies

ETHICAL DECLARATION

In this thesis study, which I have prepared in accordance with the Bolu Abant İzzet Baysal University, Institute of Graduate Studies' Thesis Writing Guide and Template:

- I have obtained the data, information, and documents presented in the thesis within the framework of academic and ethical rules.
- I have presented all information, documents, evaluations, and results in accordance with the rules of scientific ethics and morality.
- I have cited and referenced all the works I have benefited from in the thesis study.
- I have not made any changes to the data used.
- I declare that the work I have presented in this thesis is original, and in any other case, acknowledge and accept any potential loss of rights that may arise against me.

According to the similarity report obtained by applying the filters determined by the directorate of the institute in the Turnitin program related to the thesis, the similarity index of the thesis does not exceed 30%.

.....

SEDANUR DİMETOKALI

PREFACE

This thesis represents the culmination of my extensive research and academic pursuits over the past years. It focuses on the synthesis and characterization of cobalt orthoborate nanopowders, a topic of both personal significance and scientific interest. The insights and findings presented herein are the outcome of countless hours of rigorous experimentation, detailed analysis, and critical thought.

ABSTRACT

SYNTHESIS AND CHARACTERIZATION OF COBALT ORTHOBORATE NANOPOWDERS
MSC THESIS
SEDANUR DİMETOKALI
BOLU ABANT IZZET BAYSAL UNIVERSITY
INSTITUTE OF GRADUATE STUDIES
DEPARTMENT OF CHEMISTRY
(SUPERVISOR: Prof. Dr. AYŞE MORKAN)
(CO-SUPERVISOR: Dr. LISKA FADLIYANI)
BOLU, 9 APRIL 2025
x + 22 pages

This thesis study investigates the effects of various parameters on the production of nanosized cobalt borate ($Co_3(BO_3)_2$). The synthesis of nanosized cobalt borate was successfully achieved using five different fuels—glycine, beta-alanine, 1,6-diaminohexane, carbohydrazide, and hexamethylenetetramine—through a solution combustion method. The primary aim of this research is to evaluate the potential of different fuels, as well as the effects of temperature and reaction time, to exceed standard production conditions and to analyze the structural properties of the obtained materials.

During the production process, the starting materials ($Co(NO_3)_2 \cdot 6H_2O$ and H_3BO_3) and fuels were separately dissolved in pure water. The mixtures were then gelled and subjected to thermal treatment at 400°C for approximately 5-10 minutes. Following the combustion reaction, the resulting ceramic powders were reheated at 900°C for 1 hour. Characterization studies conducted using X-ray powder diffraction (XRD) and Fourier Transform Infrared Spectroscopy (FTIR) methods revealed that the production of high-purity and homogeneous nanosized cobalt borate was achieved in a very short time frame (1 hour) using the solution combustion method with all the fuels employed in this thesis.

KEYWORDS: Nanosized, Cobalt Orthoborate, $Co_3(BO_3)_2$, Solution Combustion method (SCS), XRD, FTIR spectroscopy.

ÖZET

KOBALT ORTOBORAT NANOTOZLARIN SENTEZİ VE KARAKTERİZASYONU
YÜKSEK LİSANS TEZİ
SEDANUR DİMETOKALI
BOLU ABANT İZZET BAYSAL ÜNİVERSİTESİ
LİSANSÜSTÜ EĞİTİM ENSTİTÜSÜ
KİMYA ANA BİLİM DALI
(TEZ DANIŞMANI: Prof. Dr. AYŞE MORKAN)
(İKİNCİ DANIŞMAN: Dr. LISKA FADLIYANI)
BOLU, 9 NİSAN 2025
x + 22 sayfa

Bu tez çalışması, nanoboyutlu kobalt ortoborat ($Co_3(BO_3)_2$) üretiminde kullanılan farklı parametrelerin etkisini incelemektedir. Nanoboyutlu kobalt ortoborat üretimi, çözeltide yanma yöntemi kullanılarak beş farklı yakıt—glisin, beta-alanin, 1,6-diaminoheksan, karbohidrazid ve heksametilentetramin—ile başarıyla gerçekleştirilmiştir. Bu araştırmanın temel amacı, çözeltide yanma sentez yönteminde kullanılan farklı yakıtların ve sıcaklık derecesi ile tepkime süresinin etkisinin standart üretim koşullarını aşma potansiyelini değerlendirmek ve elde edilen malzemelerin yapısal özelliklerini analiz etmektir.

Üretim sürecinde, başlangıç malzemeleri ($Co(NO_3)_2 \cdot 6H_2O$ ve H_3BO_3) ile yakıtlar ayrı ayrı saf su içinde çözülmüştür. Karışımlar daha sonra jel haline getirilmiş ve 400°C'de (yaklaşık 5-10 dakika) ısıl işleme tabi tutulmuştur. Yanma tepkimesi sürecinin ardından elde edilen seramik tozlar, 900°C'de 1 saat süreyle tekrar ısıtma işlemine tabi tutulmuştur. X-ray toz difraksiyonu (XRD) ve Fourier Dönüşüm Kızılötesi Spektroskopisi (FTIR) yöntemleri kullanılarak gerçekleştirilen karakterizasyon çalışmaları sonucunda, yüksek saflıkta ve homojen yapıya sahip nanoboyutlu kobalt ortoborat üretiminin, bu tez çalışmasında kullanılan tüm yakıtlarla uygulanan çözeltide yanma üretim yöntemi ile, çok kısa bir zaman aralığında (1 saat) gerçekleştiği görülmüştür.

ANAHTAR KELİMELER: Nano boyut, Kobalt Ortoborat, $Co_3(BO_3)_2$, Çözeltide yanma yöntemi (SCS), XRD, FTIR spektroskopi.

TABLE OF CONTENTS

Page

ABSTRACT ..... **v**

ÖZET ..... **vi**

TABLE OF CONTENTS ..... **vii**

LIST OF FIGURES ..... **viii**

LIST OF ABBREVIATIONS AND SYMBOLS……...**ix**

ACKNOWLEDGEMENT ..... **x**

1. INTRODUCTION **1**

1.1 General Information 1

1.2 Cobalt Orthoborate 3

1.2.1 Crystal Structure and Group-Theoretical Analysis of Cobalt Orthoborate 4

1.2.2 Synthesis of Cobalt Orthoborates 5

2. MATERIALS and METHOD **7**

3. RESULTS **8**

3.1 Devices Used in Characterization 8

3.1.1 Powder X-Ray Diffraction 8

3.1.2 Infrared Spectrometer (FT-IR) 8

3.2 Characterization of XRD Patterns 8

3.3 Characterization of Infrared Spectra 11

4. DISCUSSION **16**

5. CONCLUSION **19**

REFERENCES **21**

LIST OF FIGURES

Page

Figure 1.1. Crystal structure of kotoite structured metal (Metal = Mg, Co, Ni) orthoborates (Aimin et al., 2011; Knyrim, 2008; Lofland et al., 2010) 2
Figure 1.2. Structure of $Co_3(BO_3)_2$. Here Co1 and Co2 are cobalt Co^{2+} ions at the 2a and 4*f* Wyckoff positions, respectively; O1 and O2 are oxygen ions at the 4*g* and 8*h* positions; boron B is at the 4*g* positions. (Molchanova A.D. et al., 2021)..... 4
Figure 2.1. Preparation Stages of Cobalt Orthoborate, $Co_3(BO_3)_2$ Compound with Different Fuels by Solution Combustion Method (Nagendra et al., 2019)..... 7
Figure 3.1. X-ray patterns of Cobalt Orthoborate Compound Prepared by Solution Combustion Method Using Different Fuels at 400°C..... 9
Figure 3.2. X-Ray Patterns of The Cobalt Orthoborate Compound Prepared by The Solution Combustion Method Using Different Fuels At 900°C 10
Figure 3.3. FT-IR spectra of $Co_3(BO_3)_2$ Compound Produced with Fuel No. 1 at 400°C and 900°C..... 11
Figure 3.4. FT-IR spectra of $Co_3(BO_3)_2$ Compound Produced with Fuel No. 2 at 400°C and 900°C..... 12
Figure 3.5. FT-IR spectra of $Co_3(BO_3)_2$ Compound Produced with Fuel No. 3 at 400°C and 900°C..... 13
Figure 3.6. FT-IR spectra of $Co_3(BO_3)_2$ Compound Produced with Fuel No. 4 at 400°C and 900°C..... 14
Figure 3.7. FT-IR spectra of $Co_3(BO_3)_2$ Compound Produced with Fuel No. 5 at 400°C and 900°C..... 15

LIST OF ABBREVIATIONS AND SYMBOLS

^{o}C	: Centigrade
CuKα	: Copper K-alpha
FTIR	: Fourier Transform Infrared Spectroscopy
FUEL No 1	: Glycine
FUEL No 2	: Beta alanine
FUEL No 3	: 1,6-diaminohexane
FUEL No 4	: Carbohydrazide
FUEL No 5	: Hexamethylenetetramine
HMDA	: 1,6-diaminohexane
HMTA	: Hexamethyltetramine
nm	: Nanometre
SCS	: Solution Combustion Synthesis
XRD	: Xray Diffraction
λ	: Lambda

ACKNOWLEDGEMENT

I would like to express my sincere gratitude to Prof. Dr. Ayşe Morkan and Dr. Liska Fadliyani for their unwavering support during the preparation of this study. They guided me through all stages of my work with their knowledge, expertise and guidance, and their contributions were invaluable throughout the completion of this thesis.

I am also very grateful to my family for the constant encouragement and support they have given me throughout this journey. Their patience, understanding and moral support have always been a source of strength for me and they stood by me as my biggest supporters.

1. INTRODUCTION

1.1 General Information

Boron is the 51st element commonly found in the earth's crust. It is known that there are approximately 230 types of boron minerals in nature. The different properties of its compounds with various metal or nonmetal elements enable the use of boron compounds in many industrial areas (National Boron Research Institute, 2003).

The element boron is not found pure in nature, it is generally found in nature as oxygen compounds and these compounds are called borate (Beatty, 2005). Borate compounds can be classified both by the coordination number the boron atoms have and by the number of oxygen atoms shared by each BO_3 or BO_4 group. Borate compounds can consist only of planar triangular BO_3 or regular tetrahedral BO_4 anions, or they can consist of a mixture of both BO_3 and BO_4 groups (Péter et al., 2012). Borate compounds in monomer structure consisting of isolated BO_3 or BO_4 groups are called orthoborate.

In addition to naturally occurring borate compounds, there are also synthetically synthesized compounds. Different borate compounds can be obtained as a result of the reaction of some compounds containing metal and boron with each other under suitable conditions. Borate compounds; They are extremely important because they have properties such as magnetic, catalytic, optical, fluorescence, phosphorescence and luminescence (Péter et al., 2012; Chaminade et al.,1999; Zhang et al., 2002; Wu et al., 2007; Anantharamulu et al., 2008; Kumari et al., 2010; Cai et al., 2011). Therefore, recently, the preparation of metal borates with different methods has become very popular due to their use in laser applications and as cell fuel, as well as these properties (Liu et al., 2012; Sharma et al., 2011).

For example, the orthorhombic $Mg_3(BO_3)_2$ compound from metal borates was obtained by turning the starting materials into a gel by mixing the starting materials in solution with the solvothermal method and heating the resulting gel at 400°C for 6 hours. When its structure was examined, it was observed that the obtained compound was in the form of nano rods (Xu et al., 2008). In another study, flower-type $Mg_3B_2O_6$ nanoparticles were synthesized by precipitation reaction and obtained by heating at 650°C for 4 hours to complete the thermal transformation (Chen et al., 2012).

Nickel orthoborate was synthesized by Weir & Schroeder in 1964 with the formula $3NiO.B_2O_3$, and it was reported by Götz to be isomorphic with cobalt and magnesium orthoborates, but its crystal structure could not be determined at that time. Later, the crystal structure of single crystal nickel orthoborate, $Ni_3(BO_3)_2$, obtained by melting $3NiO.B_2O_3$ at 1200°C, was explained by Pardo et al. in 1974 and the cell parameters of nickel orthoborate were a=5.396, b=4.459, c= It is 8.297, has the Pnnm space group and crystallizes in the orthorhombic system, it was determined by the three-dimensional Patterson method (Pardo et al., 1974).

Effenberger and Pertlik (1984) have discovered that single crystal magnesium orthoborate, $Mg_3(BO_3)_2$, cobalt orthoborate, $Co_3(BO_3)_2$, and nickel orthoborate, $Ni_3(BO_3)_2$, crystals synthesized by the classical solid state reaction were kotoite type and that manganese orthoborate, $Mn_3BO_{3)2}$ crystal was jimboite (They also explained that it has an identical structure with kotoite) using single crystal X-ray diffraction data, in 1984. Kotoite type metal orthoborates can be written in the formula $M_3(BO_3)_2$ as well as $M_3B_2O_6$.

The crystal structure of kotoite type metal orthoborates ($M_3(BO_3)_2$) is given in figure 1.1 below. In this structure, metal atoms are at the center of regular octahedrons (green) formed by oxygen atoms. As seen in the figure, small red spheres represent oxygen atoms and boron atoms are located at the center of the plane triangular surfaces.

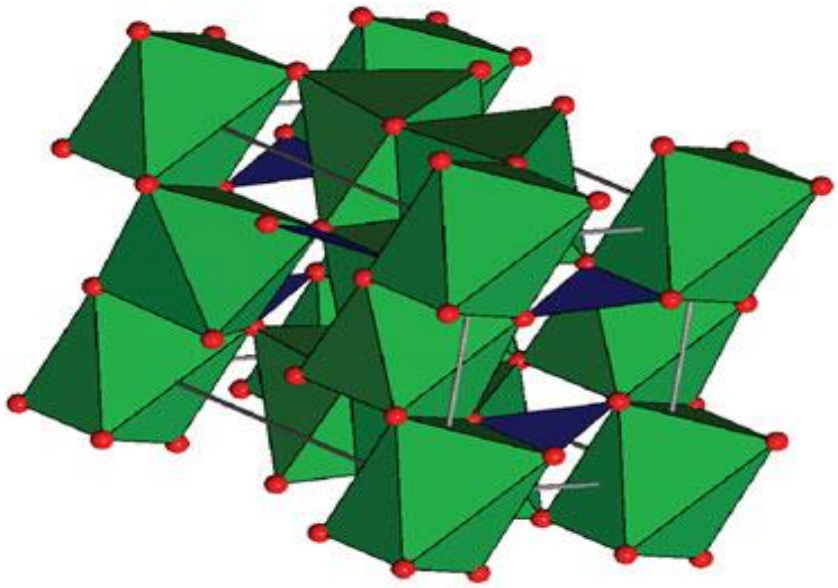

Figure 1.1. Crystal structure of kotoite structured metal (Metal = Mg, Co, Ni) orthoborates (Aimin et al., 2011; Knyrim, 2008; Lofland et al., 2010)

Orthorhombic $Me_3(BO_3)_2$ (Me= Co, Ni) kotoite compounds were synthesized by the flux method and their magnetic properties were examined. In contrast to the $Ni_3(BO_3)_2$ compound, the strong anisotropic magnetic properties of the $Co_3(BO_3)_2$ compound were detected (Bezmaternykh et al., 2012).

1.2 Cobalt Orthoborate

In recent years, transition metal borate-based compounds have attracted significant attention in crystallographic research, primarily due to the variety of structural types achievable through the trigonal or tetrahedral coordination of boron. Borate nanomaterials have gained considerable importance in the fields of electrocatalysis, sensors, and lithium-ion batteries, owing to their remarkable electrochemical properties.

A wide range of crystal structures can be observed in transition metal and rare-earth metal borates, many of which exhibit unique and intriguing physical characteristics. The complexity of these materials stems from the presence of planar $[BO_3]$ or tetrahedral $[BO_4]$ units, both of which display strong covalent B–O bonding.

Among various transition metal borates, cobalt borates appear to be the least extensively studied. The cobalt borate oxide system is known to exhibit diverse structures depending on its composition. For instance, different structural types include ludwigite-type $Co_3(BO_3)_2O_2$ (a mineral analogous to $Mg_2Fe(BO_3)O_2$), pyroborate ($Co_2B_2O_5$), tetraborate (CoB_4O_7), metaborate ($Co_4(BO_2)_6O$), and kotoite-type orthoborate $Co_3(BO_3)_2$ (Molchanova et al., 2021).

A unifying feature among these compounds is the presence of highly covalent B–O bonds, either within $[BO_3]^{2-}$ groups—as found in tetra- and metaborates—or as part of continuous –O–B–O– frameworks. While the ludwigite structure incorporates cobalt in mixed oxidation states (Co^{3+}/Co^{2+}), all other cobalt-based oxyborates contain cobalt exclusively in the divalent Co^{2+} state (Molchanova et al., 2021).

Materials known as transition metal oxyborates—particularly those with the general formula $M_3(BO_3)_2$, where M = Mn, Co, or Ni—form a class of compounds typically characterized by the kotoite-type crystal structure (Somanath et al., 2023).

A kotoite-type $Co_3(BO_3)_2$ crystal structure was synthesized via a two-step solid-state thermal treatment and was successfully employed as an electrocatalyst

for water oxidation under neutral conditions (Turhan et al., 2018). Additionally, single crystals of $Co_3(BO_3)_2$ have been grown using the flux method (Molchanova et al., 2021).

1.2.1 Crystal Structure and Group-Theoretical Analysis of Cobalt Orthoborate

The orthoborate $Co_3(BO_3)_2$ crystallizes in the same structure as the kotoite mineral $Mg_3(BO_3)_2$, in which the nonmagnetic Mg^{2+} ion can be substituted by magnetic Ni^{2+} or Mn^{2+} ions (Figure 1.2). The crystal belongs to the orthorhombic space group *Pnnm* (No. 58, Z = 2), with a point group symmetry of *mmm* (D_2h). There are two formula units per primitive unit cell. Using the standard axis setting of $a < b < c$, the lattice parameters are: a = 4.5 Å, b = 5.4 Å, and c = 8.3 Å. In this setting, the Cartesian coordinates x, y, and z correspond to the crystallographic axes *a*, *b*, and *c*, respectively.

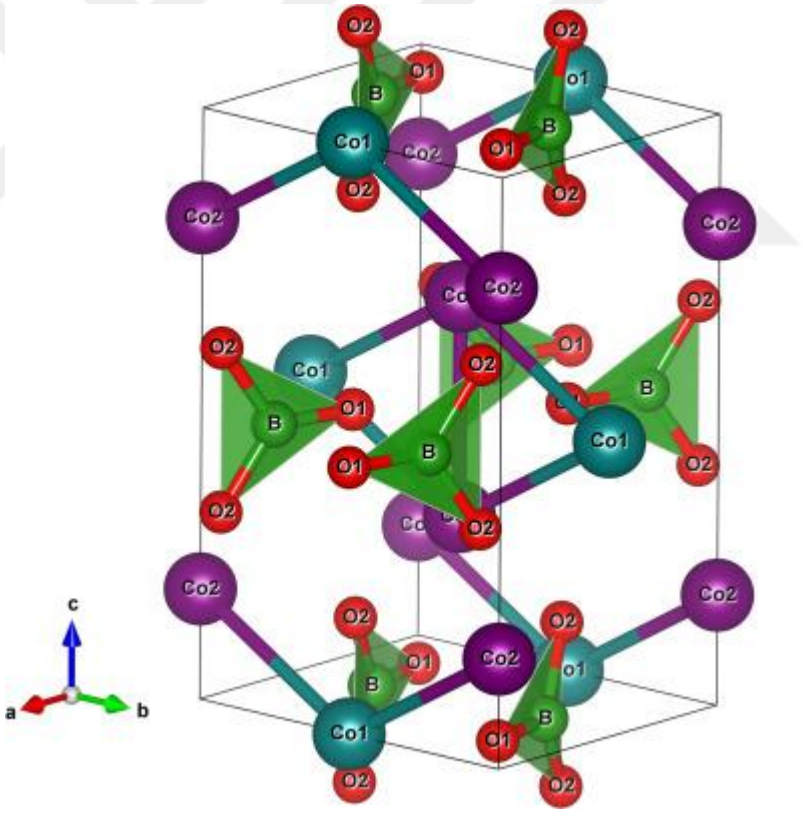

Figure 1.2. Structure of $Co_3(BO_3)_2$. Here Co1 and Co2 are cobalt Co^{2+} ions at the 2a and 4*f* Wyckoff positions, respectively; O1 and O2 are oxygen ions at the 4*g* and 8*h* positions; boron B is at the 4*g* positions. (Molchanova A.D. et al., 2021)

1.2.2 Synthesis of Cobalt Orthoborates

As it is known, technology is advancing day by day with the developments in the scientific field, and the scientific world benefits most from this progress. The development of devices used in the scientific field, the materials used in synthesis being more durable and purer, and the existence of new devices with which we can examine their morphologies allow the scientific world to go one step further every day. As a result of these developments, the effect of even the smallest change in the method on the result can be easily examined, and thus, it is possible to obtain purer and superior substances compared to the past.

Recently, the scientific world has been progressing towards making existing materials more durable and having superior properties by developing them with new methods rather than searching for new materials. Because the electronic devices we use in daily life increasingly take up a larger place in our lives, the importance of providing optical properties to materials that will meet the appropriate conditions has increased. Therefore, recent research has focused on synthesizing new borates, characterizing them, and examining their optical and luminescence properties. It has been noticed that morphological changes occur in the structure of the substance even when the synthesis method is changed, and it is seen in the studies conducted in the literature that these morphological features affect all the physical behaviors of the substance.

The physical behavior of materials is defined by various electrical, magnetic, optical, thermal and elastic properties. These properties are mostly directly related to the atomic structure, atomic arrangement, crystal structure of the material and the purity of the material, and it is generally seen that these properties are hindered by the emergence of undesirable phases due to the compounds synthesized by classical methods remaining at high temperatures for a long time. For this reason, it is aimed to eliminate such problems by obtaining high purity substances by using new synthesis methods such as the combustion method.

In the literature study, the properties, synthesis conditions and fabrication methods of these borate compounds were examined, and the synthesis of cobalt orthoborates via the solution combustion method has been rarely reported in the literature. Most recently, Beena et al., 2025, documented the successful preparation of these compounds using glycine as a fuel in this method. Accordingly, their approach demonstrates the potential of solution combustion synthesis (SCS) as a

simple, cost-effective, and energy-efficient route for obtaining phase-pure cobalt orthoborates. The use of glycine, which acts both as a fuel and complexing agent, facilitates a self-sustaining exothermic reaction that leads to rapid crystallization of the desired product.

This method offers several advantages over conventional solid-state synthesis, including lower reaction temperatures, shorter synthesis durations, and improved control over particle morphology. However, despite these promising features, the SCS technique remains under explored for borate systems, especially for cobalt-based orthoborates. Therefore, further investigations into the optimization of reaction parameters such as fuel-to-oxidizer ratio, type of fuel, and annealing conditions could significantly enhance the understanding and applicability of this method for borate materials.

The combustion technique in solution is an extremely important synthesis technique, as it allows substances to be synthesized extremely quickly and ensures that the compounds have a high surface area, high purity and homogeneous structure (Kingsley & Patil, 1988). Within the scope of this thesis, the solution combustion method was used to produce nano-sized cobalt orthoborate compounds using five different organic fuels (Glycine, Beta alanine, 1,6-diaminohexane, Carbohydrazide, Hexamethylenetetramine). Characterization of the materials obtained was made using X-ray powder diffraction and Fourier Transform infrared spectroscopy techniques.

2. MATERIALS and METHOD

The solution combustion technique is a new synthesis method that allows extremely rapid synthesis of materials. The process is used to synthesize complex compounds by mixing a metal source (oxidant) in the form of nitrate in a stoichiometric ratio and a fuel (reducer) (e.g. hydrazine, urea or glycine) in water and heating it in a single-stage process as a result of automatic ignition.

The advantage of this technique is that the structural parameters of the synthesized product can be controlled by changing the reactant and fuel ratio and composition. Another advantage of this technique is that the substance synthesized at low temperature and in a very short time has a high surface area, high purity and homogeneous structure (Kingsley & Patil, 1988).

In this research, $Co(NO_3)_2.6H_2O$, H_3BO_3 starting materials and different fuels (1. Glycine, 2. Beta alanine, 3. 1,6-diaminohexane, 4. Carbohydrazide, 5. Hexamethylenetetramine) were used for the synthesis. Figure 2.1 shows the preparation stages of Cobalt Orthoborate Compound with different fuels using the Solution Combustion Method.The starting materials and fuel in stoichiometric proportions were dissolved in pure water and the water was evaporated until a gel-like mixture was obtained. The resulting mixture was then placed in the oven and combustion occurred, and the powders, which were taken out of the oven and ground homogeneously, were subjected to high temperature heat treatment in the oven again to complete the thermal transformation. Then, the characterization of the obtained products was made by XRD and FTIR methods.

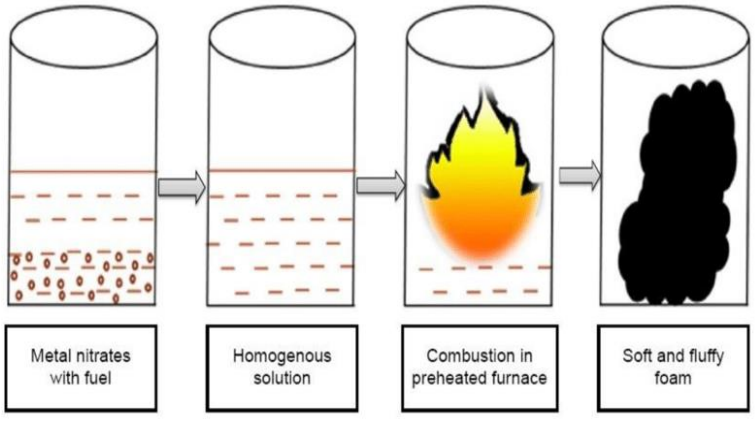

Figure 2.1. Preparation Stages of Cobalt Orthoborate, $Co_3(BO_3)_2$ Compound with Different Fuels by Solution Combustion Method (Nagendra et al., 2019)

3. RESULTS

3.1 Devices Used in Characterization

3.1.1 Powder X-Ray Diffraction

Powder X-ray diffraction (XRD) patterns required for structural analysis of the synthesized materials were obtained using Rigaku multiflex, BD127412, model XRD device. The scanning process was carried out between 6.00º and 70.00º 2θ angles (CuKα, (λ=1.54056 Å)).

Then, using the Debye-Scherrer equation below, the crystallite sizes of the obtained compounds were determined by X-ray patterns (Scherrer, 1918; Patterson, 1939; Chandrappa and Venkatesha, 2012).

$$t = \frac{K\lambda}{\beta cos\theta}$$

(t: crystallite size (nm), K structure factor and is usually taken as 0.9, λ=1.5406 is wavelength (CuKα), β is (radian) and θ is Bragg angle)

3.1.2 Infrared Spectrometer (FT-IR)

Infrared spectra were taken with a Shimadzu model device in the wavelength range of 400-4000 cm^{-1}.

3.2 Characterization of XRD Patterns

In this study, the production of $Co_3(BO_3)_2$ compound by the solution combustion synthesis method, which is explained in detail in the synthesis method section, was successfully carried out using different fuels. For the synthesis, other starting materials, except boric acid (4% excess), were used in stoichiometric proportions. The calculated starting materials were weighed, dissolved in water, and then turned into a gel using a heater. The resulting gel was placed in an oven at 400ºC for 5 minutes, where the combustion reaction was carried out and powder material was obtained. The obtained powder materials were heated at 900 ºC for 1 hour to complete the heat treatment. Phase analyzes of borate materials obtained at 900 ºC were performed using X-ray powder pattern data. XRD patterns of the obtained cobalt borates are given in Figures 3.1 and 3.2, respectively. In XRD patterns; fuel 1 : red XRD; fuel 2 : green XRD; fuel 3 : gray XRD; fuel 4 : purple XRD ; fuel 5 corresponds to yellow XRD.

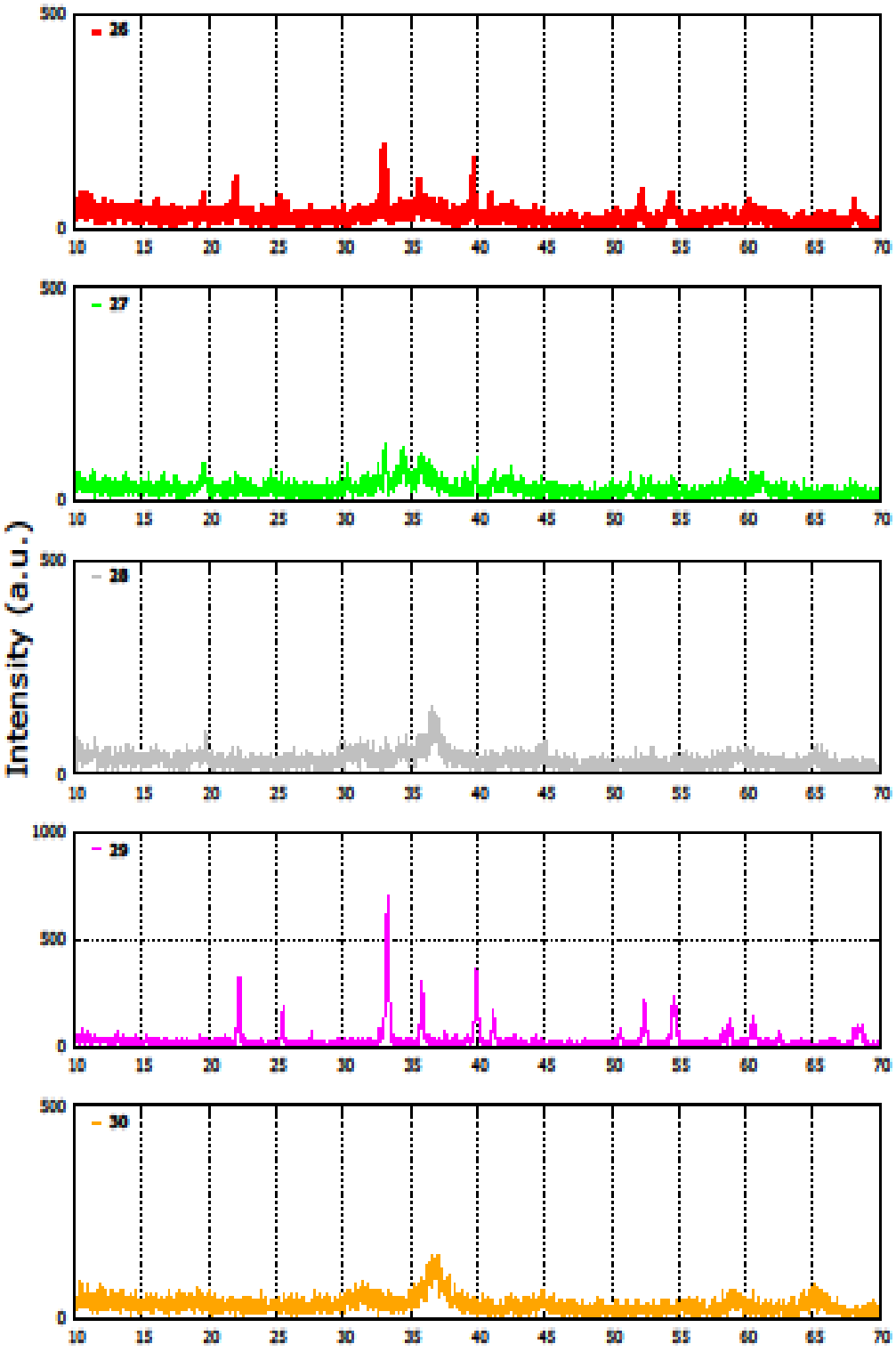

Figure 3.1. X-ray patterns of Cobalt Orthoborate Compound Prepared by Solution Combustion Method Using Different Fuels at 400°C.

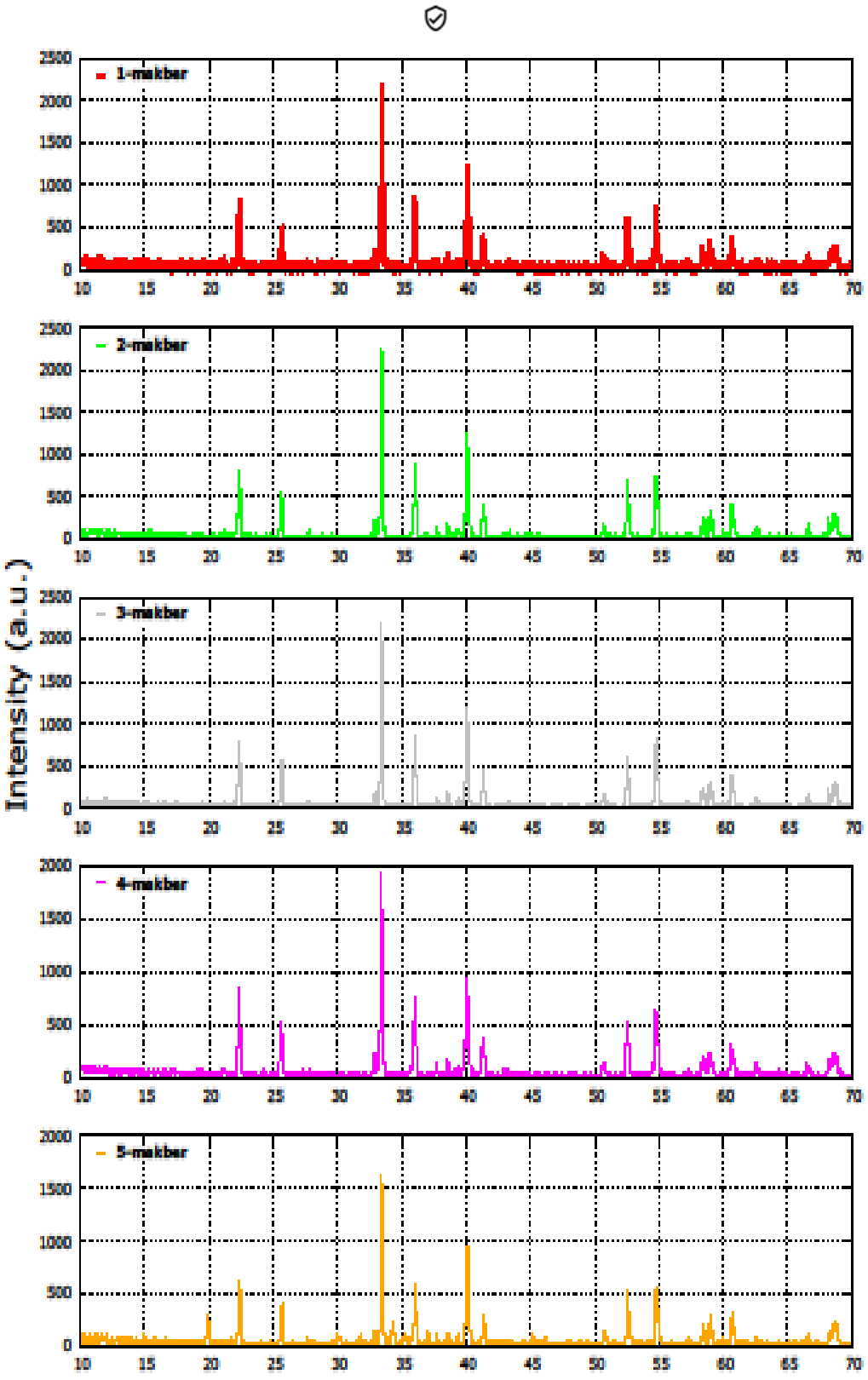

Figure 3.2. X-Ray Patterns of The Cobalt Orthoborate Compound Prepared by The Solution Combustion Method Using Different Fuels At 900°C

3.3 Characterization of Infrared Spectra

The infrared spectra of the products obtained are given in Figures 3.3 to Figure 3.7. When the infrared spectra are examined, it is seen that there are vibration bands belonging to the cobalt orthoborate, $Co_3B_2O_6$, compound in the kotoite structure, parallel to the XRD patterns.

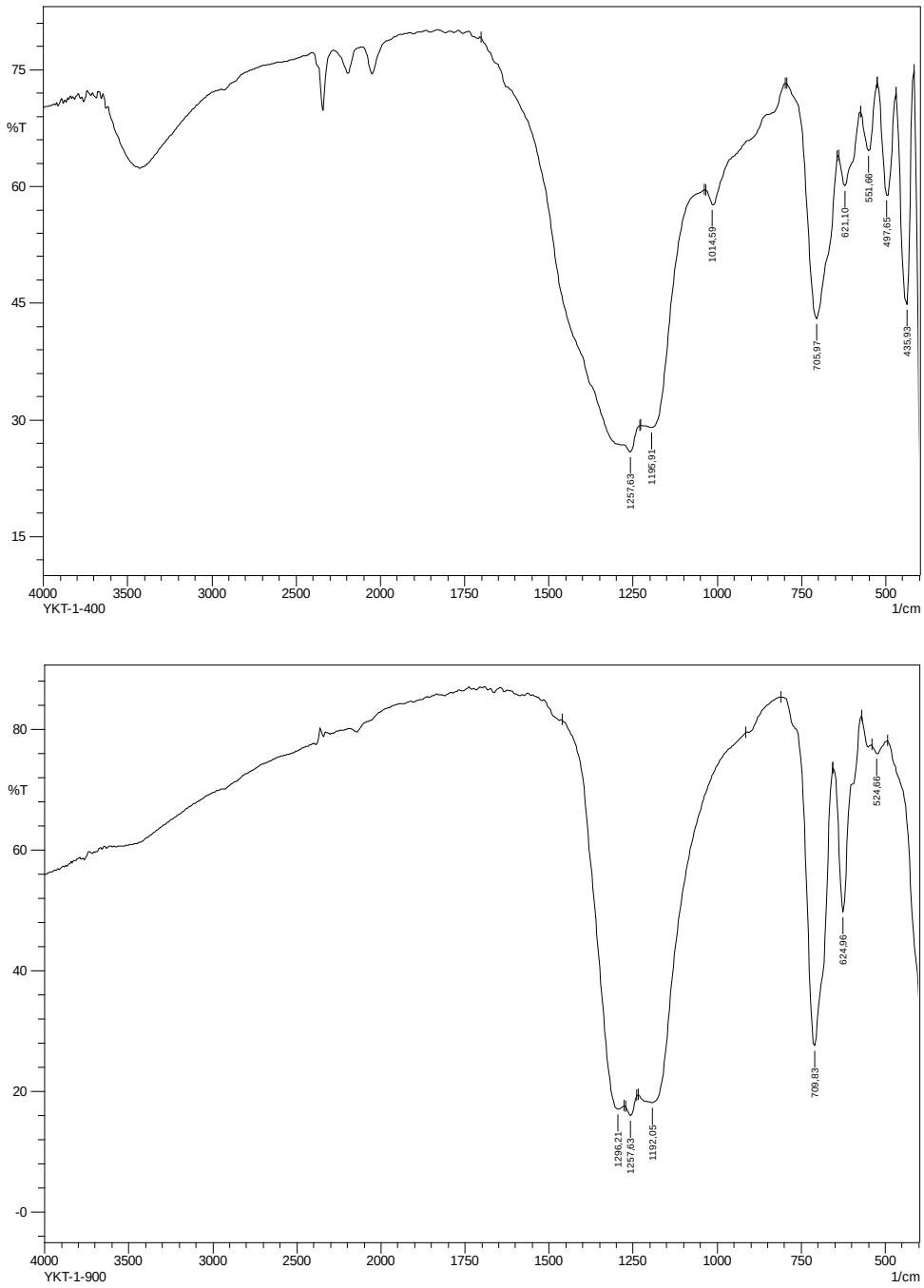

Figure 3.3. FT-IR spectra of $Co_3(BO_3)_2$ Compound Produced with Fuel No. 1 at 400°C and 900°C

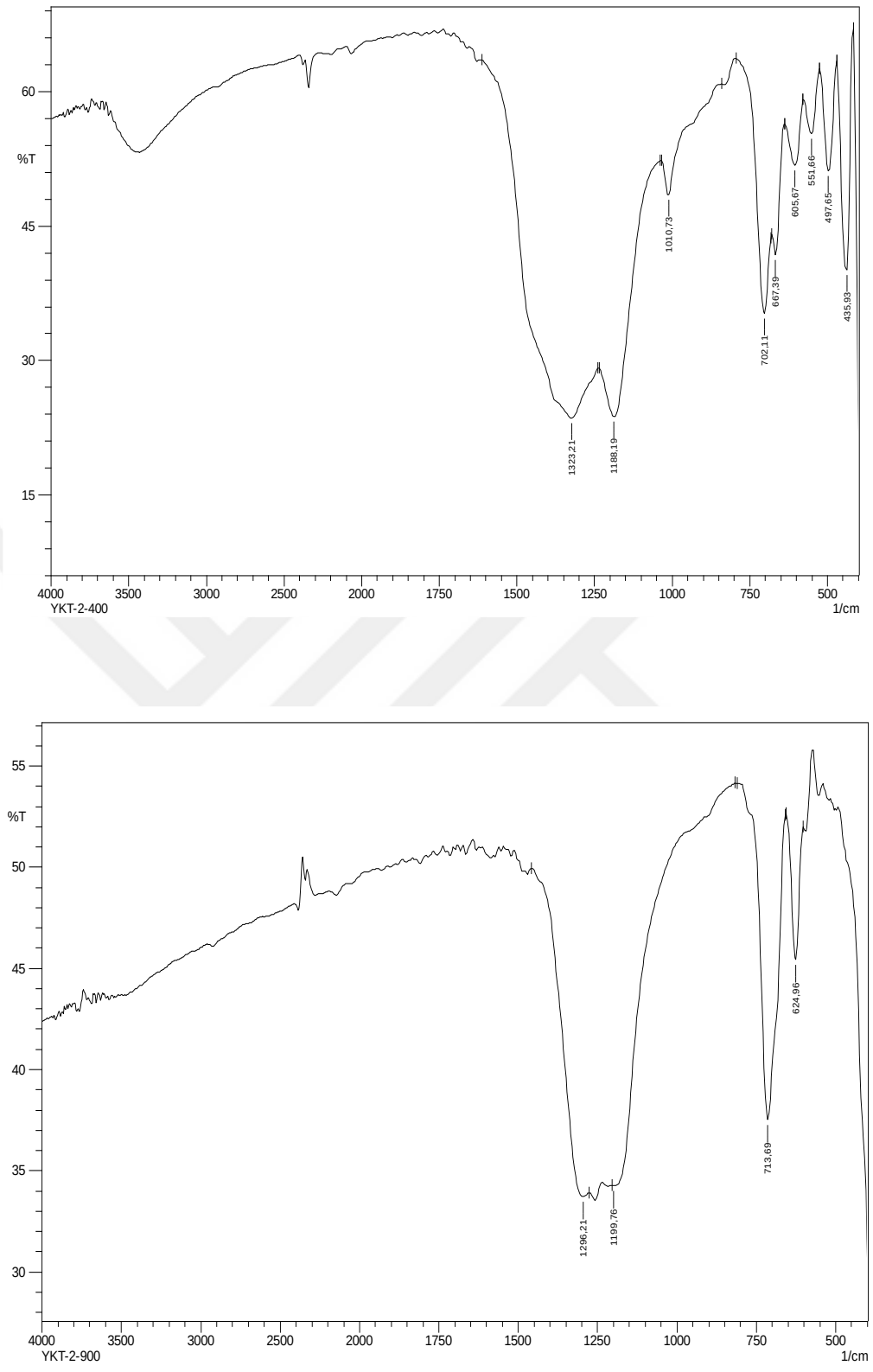

Figure 3.4. FT-IR spectra of $Co_3(BO_3)_2$ Compound Produced with Fuel No. 2 at 400°C and 900°C

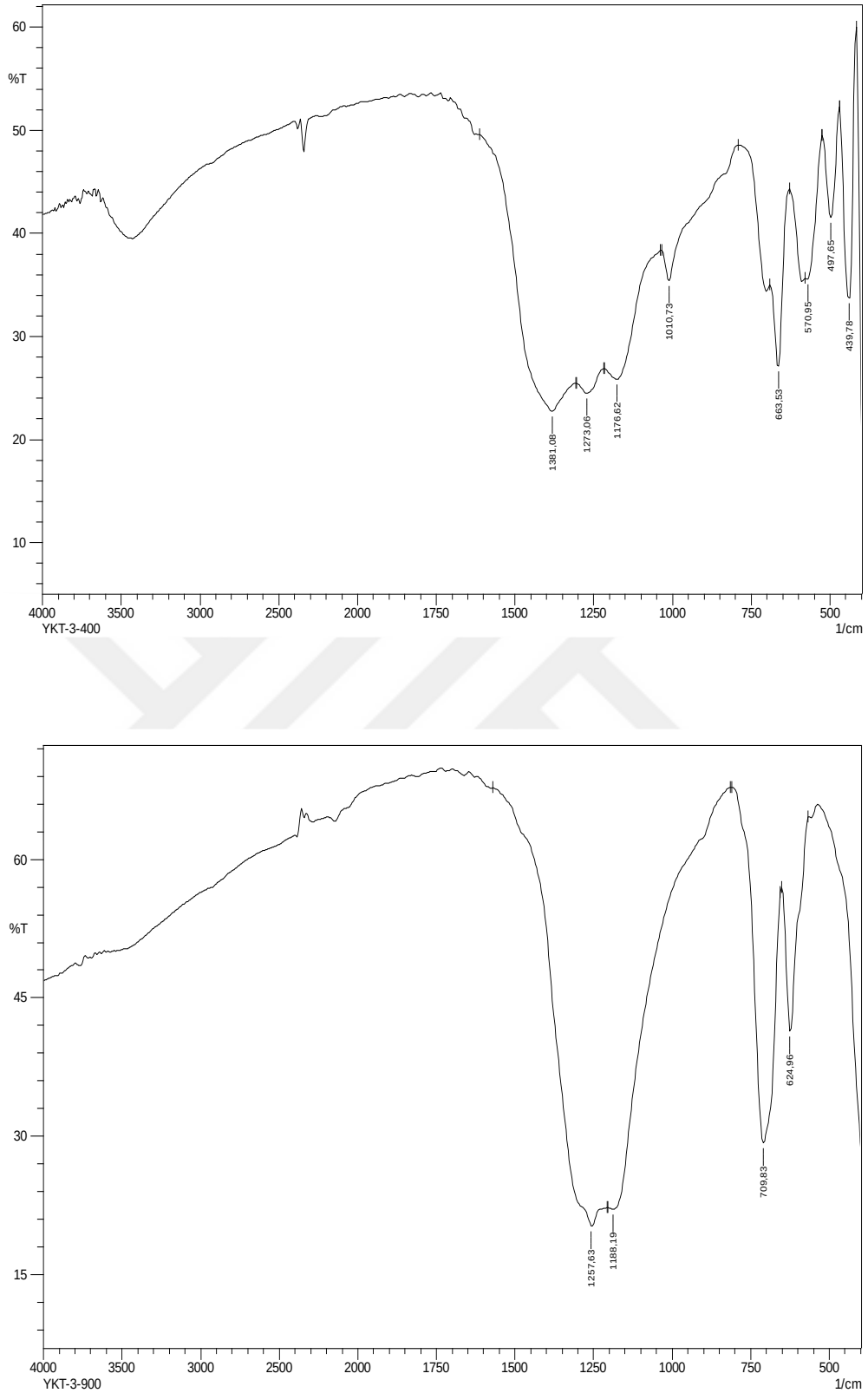

Figure 3.5. FT-IR spectra of $Co_3(BO_3)_2$ Compound Produced with Fuel No. 3 at 400°C and 900°C

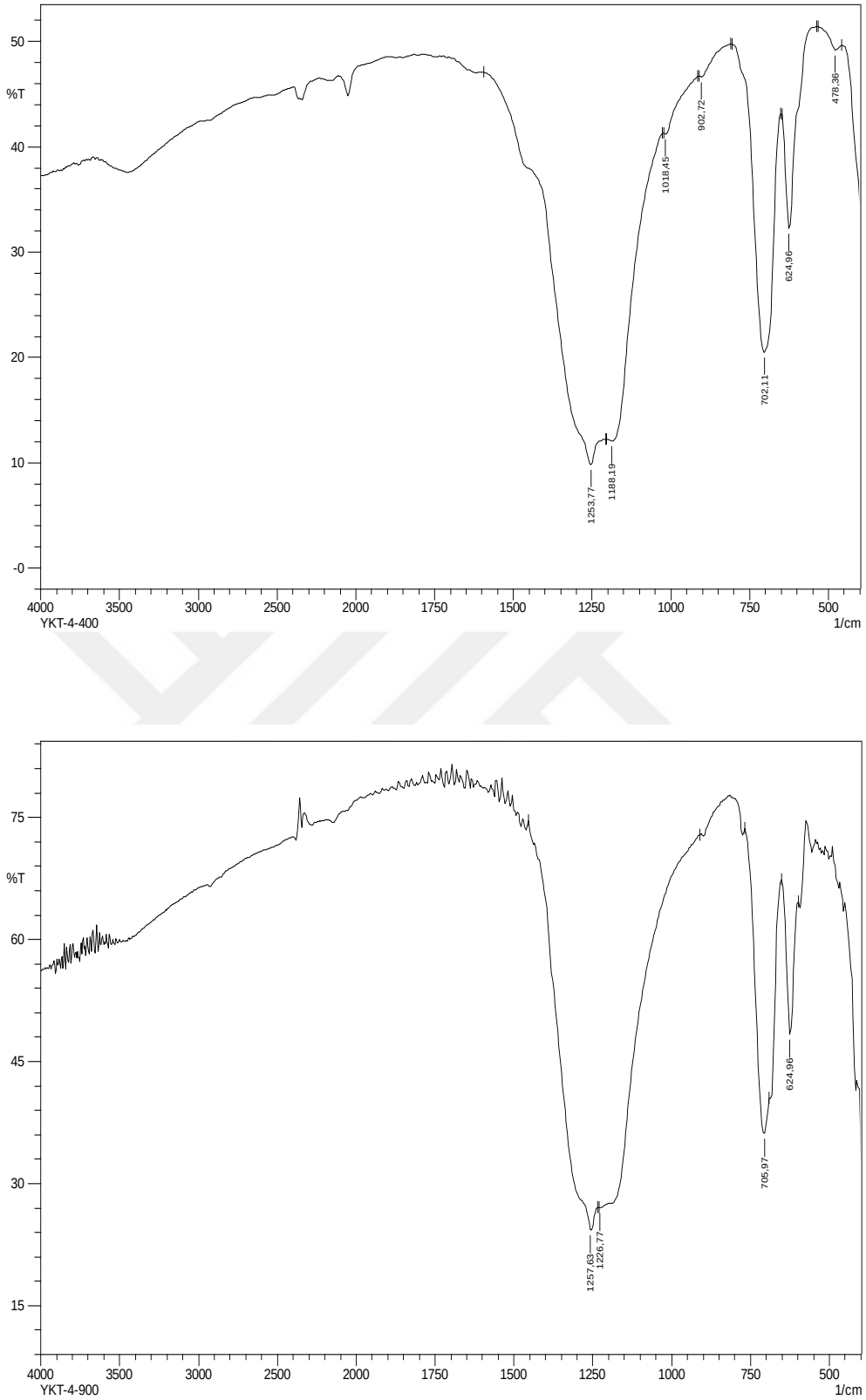

Figure 3.6. FT-IR spectra of $Co_3(BO_3)_2$ Compound Produced with Fuel No. 4 at 400°C and 900°C

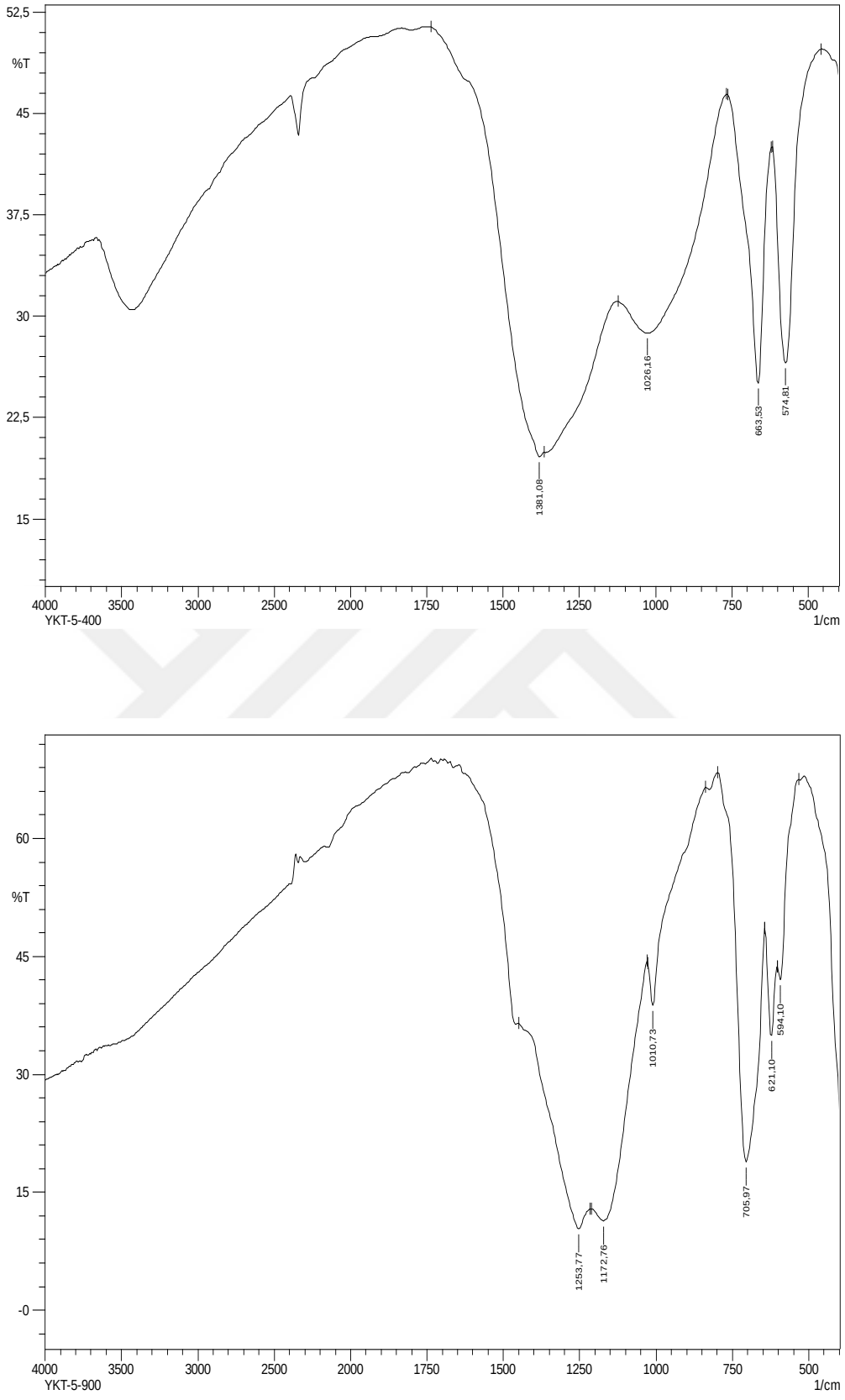

Figure 3.7. FT-IR spectra of $Co_3(BO_3)_2$ Compound Produced with Fuel No. 5 at 400°C and 900°C

4. DISCUSSION

The analysis of the X-ray diffraction (XRD) patterns reveals that cobalt orthoborate with a kotoite-type structure was successfully synthesized in a single phase. All observed diffraction peaks correspond exclusively to the kotoite phase, $Co_3(BO_3)_2$ (ICDD card no: 25-0102), with no evidence of secondary phases. This indicates that the use of different fuel types during synthesis did not alter the structural integrity of the kotoite structure. Consequently, it can be concluded that the kotoite structure was preserved without decomposition, and the synthesis procedure was effectively controlled.

A detailed examination of the X-ray diffraction (XRD) patterns presented in Figure 3.1 reveals distinct differences in the structural properties of the synthesized materials depending on the type of fuel used during the combustion synthesis process. Specifically, the samples prepared using fuels numbered 1, 2, 3, and 5 exhibited broad and diffuse diffraction profiles, characteristic of an amorphous structure. The absence of sharp diffraction peaks in these samples suggests that the energy released during combustion was insufficient to promote the long-range atomic ordering required for crystallization under the initial synthesis conditions. In contrast, the material obtained using fuel no. 4 displayed well-defined diffraction peaks, indicative of a crystalline phase. This difference underscores the critical role of fuel characteristics—such as combustion temperature, reaction enthalpy, and gas evolution rate—in influencing the thermal environment and, consequently, the degree of crystallinity during synthesis.

In Figure 3.2, which presents the XRD patterns of the same samples after a thermal treatment at 900 °C, it is observed that all fuel types ultimately yielded products with a crystalline cobalt orthoborate ($Co_3(BO_3)_2$) structure. The emergence of sharp and well-resolved peaks across all samples demonstrates that high-temperature calcination effectively induces a phase transformation from an initially amorphous state to a crystalline ceramic phase. This transformation indicates that, regardless of the initial structural differences resulting from fuel selection, thermal energy at elevated temperatures facilitates atomic diffusion and crystal nucleation processes, leading to the formation of a thermodynamically stable cobalt borate phase.

To further investigate the crystalline characteristics of the synthesized materials, the Debye–Scherrer equation was applied to the most intense diffraction peaks in each pattern to estimate the average crystallite size. The analysis revealed that the crystallite sizes of all samples calcined at 900 °C were within a narrow range of approximately 37 to 38 nanometers. This relatively uniform crystallite size distribution suggests that the thermal conditions applied were sufficient to overcome kinetic barriers to crystal growth and enabled consistent nanocrystalline development, regardless of the initial fuel composition.

Moreover, a comparative analysis of the XRD patterns in Figure 3.2 highlights notable differences in the relative degrees of crystallinity among the samples. Crystallinity, in this context, can be assessed based on the intensity and sharpness of the diffraction peaks. The sample synthesized with fuel no. 2 exhibited the most pronounced and narrow diffraction peaks, indicating the highest degree of crystallinity. This result suggests that fuel no. 2 may have provided an optimal combustion profile—potentially in terms of flame temperature, burn duration, or gas evolution—that favored the formation of well-ordered crystalline domains during synthesis and subsequent calcination. Conversely, the sample prepared with fuel no. 5 showed broader and less intense diffraction peaks, signifying the lowest crystallinity among the set. This could be attributed to suboptimal combustion behavior, possibly resulting in incomplete reaction, insufficient heat distribution, or the formation of structural defects that persisted even after calcination.

In conclusion, these findings collectively demonstrate that both the type of fuel used during combustion synthesis and the application of post-synthesis thermal treatment play crucial roles in determining the structural characteristics of cobalt orthoborate ceramics. While the initial fuel choice can influence the short-range structural organization and intermediate reaction pathways, high-temperature processing acts as a unifying step that promotes crystallization and phase purity. The systematic variation in crystallinity and the relatively consistent nanocrystalline sizes observed across the samples further emphasize the interplay between synthesis parameters and material structure in the development of functional ceramic materials.

In the interpretation of infrared (IR) spectra of borate-based compounds, the vibrational features are typically concentrated within the spectral range of 2000–500 cm^{-1}, reflecting the characteristic modes of boron-oxygen bonding in various

structural units. These vibrational modes are generally categorized into three primary regions based on the coordination geometry of the boron atoms. The first region, located between 1200 and 1600 cm^{-1}, is attributed to the asymmetric stretching vibrations of B–O bonds within trigonal planar BO_3 units. These vibrations are particularly significant as they provide direct insight into the presence and behavior of the planar borate species within the crystal structure. The second region, which spans from 800 to 1200 cm^{-1}, corresponds to the stretching vibrations of B–O bonds in tetrahedrally coordinated BO_4 units. The identification of bands in this region is indicative of the presence of more complex borate frameworks, and their intensity and position may vary depending on the degree of polymerization or the specific local environment of the BO_4 groups. The third region, typically found around 700 cm^{-1} and below, includes bending modes, particularly those associated with B–O–B linkages, which are essential for understanding the connectivity and dimensionality of the borate network. These assignments are consistent with findings reported in the literature (Akhamanova, 1962; Chen et al., 2010; Lakshminarayana & Buddhudu, 2005; Ternane et al., 2002; Tukia et al., 2005).

In light of the FTIR results obtained in this study, several distinct vibrational bands were observed that are characteristic of the kotoite phase ($Co_3(BO_3)_2$). Notably, the bands located at 1278 and 1196 cm^{-1} are associated with the asymmetric stretching vibrations of B–O bonds in BO_3 units, confirming the presence of these planar borate groups in the synthesized material. Additionally, vibrational bands detected at 724, 664, 611, 496, and 420 cm^{-1} are attributed to B–O and B–O–B bond vibrations, indicating the structural complexity and integrity of the borate framework within the kotoite phase. These bands collectively suggest a well-defined borate structure that remains consistent with the expected vibrational characteristics of $Co_3(BO_3)_2$. Furthermore, a broad absorption band observed in the high-frequency region between 3200 and 3600 cm^{-1} is ascribed to the O–H stretching vibrations, which are likely due to moisture content or water molecules associated with the potassium bromide (KBr) matrix used during pellet preparation for IR measurements. This feature, although not directly related to the borate structure itself, is commonly encountered in FTIR spectra and must be taken into consideration when interpreting results (Lakshminarayana & Buddhudu, 2005). Overall, the FTIR analysis provides comprehensive evidence supporting the formation and structural stability of the kotoite phase in the synthesized samples.

5.CONCLUSION

In the present study, nanoscale cobalt orthoborate ($Co_3(BO_3)_2$) was successfully synthesized via a solution combustion method using five different fuel types: glycine, beta-alanine, 1,6-diaminohexane, carbohydrazide, and hexamethylenetetramine. The structural properties and bonding characteristics of the synthesized materials were systematically investigated using X-ray diffraction (XRD) and Fourier-transform infrared (FTIR) spectroscopy.

XRD analysis confirmed that all synthesized samples, upon calcination at 900 °C, crystallized into a single-phase kotoite-type $Co_3(BO_3)_2$ structure, in excellent agreement with the standard diffraction pattern (ICDD no: 25-0102). At a lower synthesis temperature of 400 °C, samples prepared using glycine, beta-alanine, 1,6-diaminohexane, and hexamethylenetetramine were found to be amorphous, while the sample synthesized with carbohydrazide displayed clear crystalline features, indicating a more vigorous combustion process. Upon calcination at 900 °C, all samples underwent successful phase transformation into crystalline cobalt orthoborate. The crystallite sizes, estimated using the Debye–Scherrer equation, ranged narrowly between 37 and 38 nm, suggesting homogeneous nanostructured domains. Among the five fuels, the sample synthesized using beta-alanine exhibited the highest degree of crystallinity, whereas the sample prepared with hexamethylenetetramine showed the lowest.

FTIR spectroscopy further supported the XRD findings by confirming the presence of characteristic vibrational modes associated with the borate structure. Specifically, bands at 1278 and 1196 cm^{-1} were assigned to the asymmetric stretching vibrations of B–O bonds in the BO_3 units, characteristic of the kotoite phase. Additional vibrational bands corresponding to B–O–B linkages and tetrahedral BO_4 units were also observed in the lower wavenumber region, reinforcing the structural assignment.

Together, the XRD and FTIR results demonstrate a strong correlation between fuel type, synthesis temperature, and the structural evolution of cobalt orthoborate. The findings highlight that while high-temperature calcination ensures complete phase formation and crystallization, the nature of the fuel significantly influences combustion dynamics, which in turn affects the degree of crystallinity and structural ordering in the final product.

These results provide valuable insight for optimizing combustion synthesis parameters in the tailored preparation of borate-based ceramic materials with desired structural properties.

REFERENCES

Aimin, C., Fengchao, H., Pei, G., & Zheming, N. (2011). Sol-gel synthesis, characterization of nickel borate nanorods. *Chinese Journal of Inorganic Chemistry*, *27*, 30-34.

Akhamanova, M. V. (1962). Investigation of the structure of native borates by infrared absorption spectroscopy. *Journal of Structural Chemistry*, *3*, 24-29.

Anantharamulu, N., Vijaya, Kumar, B., Rama Devi, V., Vithal, M., (2008). Preparation, characterization and spectral studies of $Cr_{1-x}EuBO_3$ (x=0, 0.01, 0.05). *Material chemistry and physics, 108, 2-3*, 319-324.

Beatty, R. (2005). *Boron*. Marshall Cavendish.

Beena, S., Chandresh Kumar Rastogi, Yash Athreya , Shwetha, K. P., Abraham, N., Suresh Babu Viswanathan, Sudha Kamath, M. K, Manjunatha, C. (2025). Unveiling the supercapattery behaviour of novel kotoite-type $Co_3(BO_3)_2$ nanoparticles . *Journal of Energy Storage*, 110, 115299

Bezmaternykh, L. N., Sofronova, S. N., Volkov, N. V., Eremin, E. V., Bayukov, O. A., Nazarenko, I. I., & Velikanov, D. A. (2012). Magnetic properties of $Ni_3B_2O_6$ and $Co_3B_2O_6$ single crystals. *physica status solidi (b)*, *249*(8), 1628-1633.

Cai, G. M., Tao, X. M., Su, L. M., Zheng, F., Yi, D. Q., Chen, X. L., & Jin, Z. P. (2011). Structure, thermal stability and properties of $Li_3Sc(BO_3)_2$. *Journal of Solid State Chemistry*, *184*(1), 115-122.

Chaminade, J. P., Gravereau, P., Jubera, V., & Fouassier, C. (1999). A new family of lithium rare-earth oxyborates, $LiLn_6O_5$ $(BO_3)_3$ (Ln= Pr–Tm): crystal structure of the gadolinium phase $LiGd_6O_5$ $(BO_3)_3$. *Journal of Solid State Chemistry*, *146*(1), 189-196.

Chen, A. M., Gu, P., & Ni, Z. M. (2012). 3D flower-like magnesium borate microspheres assembled by nanosheets synthesized via PVP-assisted method. *Materials Letters*, *68*, 187-189.

Chen, X., Yin, H., Chang, X., Zang, H., & Xiao, W. (2010). Synthesis, crystal structure, spectrum properties, and electronic structure of a novel non-centrosymmetric borate, $BiCd_3(AlO)_3(BO_3)_4$. *Journal of Solid State Chemistry*, *183*(12), 2910-2916.

Effenberger, H., & Pertlik, F. (1984). Verfeinerung der kristallstrukturen der isotypen verbindungen $M_3(BO_3)_2$ mit M= Mg, Co und Ni (strukturtyp: kotoit). *Zeitschrift für Kristallographie-Crystalline Materials*, *166*(1-4), 129-140.

Kingsley, J. J., & Patil, K. C. (1988). A novel combustion process for the synthesis of fine particle α-alumina and related oxide materials. *Materials letters*, *6*(11-12), 427-432.

Knyrim, J. S. (2008). *Synthetic investigations of main group and transition metal borates at extreme conditions* (Doctoral dissertation, lmu).

Kumari, L., Li, W. Z., Kulkarni, S., Wu, K. H., Chen, W., Wang, C., & Leblanc, R. M. (2010). Effect of surfactants on the structure and morphology of magnesium borate hydroxide nanowhiskers synthesized by hydrothermal route. *Nanoscale research letters*, *5*, 149-157.

Lakshminarayana, G., & Buddhudu, S. (2005). Spectral analysis of Cu^{2+}: B_2O_3–ZnO–PbO glasses. *Spectrochimica Acta Part A: Molecular and Biomolecular Spectroscopy*, *62*(1-3), 364-371.

Liu, X., Zhu, W., Cui, X., Liu, T., & Zhang, Q. (2012). Facile thermal conversion route synthesis, characterization, and optical properties of rod-like micron nickel borate. *Powder technology*, *222*, 160-166.

Lofland, S. E., Ramanujachary, K. V., & Ganguli, A. K. (2010). A new low temperature methodology to obtain pure nanocrystalline nickel borate. *Journal of Organometallic Chemistry*, *695*(7), 1002-1005.

Molchanova, A. D, Prosnikov, M. A, Petrov, V. P., Dubrovin, R. M., Nefedov, S. G., Chernyshov, D., Smirnov, A. N., Davydov, V. Yu., Boldyrev, K. N., Chernyshev, V. A., Pisarev, R.V., Popova, M. N. (2021). Lattice dynamics of cobalt orthoborate $Co_3(BO_3)_2$ with kotoite structure. *Journal of Alloys and Compounds*, 865, 158797.

Nagendra, G. K., B W Shivaraj, B. W., Manjunatha, C., Ayeesha Siddiqua, S. A., and Suchithra, V. (2019). Study of structural features and antibacterial property of ZnO/CuO nanocomposites derived from solution combustion synthesis. *IOP Conf. Series: Materials Science and Engineering*, 577, 012111

National Boron Research Institute. (2003). http://www.boren.gov.tr/icerik.php?id=24 (Accessed November 28, 2024)

Pardo, J., Martinez-Ripoll, M., & Garcia-Blanco, S. (1974). The crystal structure of nickel orthoborate, $Ni_3(BO_3)_2$. *Structural Science*, *30*(1), 37-40.

Péter, A., Polgár, K., & Tóth, M. (2012). Synthesis and crystallization of lithium-yttrium orthoborate $Li_6Y(BO_3)_3$ phase. *Journal of crystal growth*, *346*(1), 69-74.

Sharma, S., Ramanujachary, K. V., Lofland, S. E., & Ganguli, A. K. (2011). Controlling the size and morphology of anisotropic nanostructures of nickel borate using microemulsions and their magnetic properties. *Journal of colloid and interface science*, *360*(2), 393-397.

Scherrer P (1918) "Nachrichten von der Gesellschaft der Wissenschaften zu Göttingen, Mathematisch-Physikalische Klasse"

Ternane, R., Cohen-Adad, M. T., Panczer, G., Goutaudier, C., Kbir-Ariguib, N., Trabelsi-Ayedi, M., & Massiot, D. (2002). Introduction of boron in hydroxyapatite: synthesis and structural characterization. *Journal of Alloys and Compounds*, *333*(1-2), 62-71.

Tukia, M., Hölsä, J., Lastusaari, M., & Niittykoski, J. (2005). Eu^{3+} doped rare earth orthoborates, RBO_3 (R= Y, La and Gd), obtained by combustion synthesis. *Optical Materials*, *27*(9), 1516-1522.

Turhan, E. A., Nune, S.V.K., Ülker, E., Şahin, U., Dede, Y., Karadas, F. (2018). Water oxidation electrocatalysis with a cobalt-borate-based hybrid system under neutral conditions. *Chem. Eur. J.*, 24 (41), 10372-10382.

Wu, L., Zhang, Y., Kong, Y. F., Sun, T. Q., Xu, J. J., & Chen, X. L. (2007). Structure determination of novel orthoborate $NaMgBO_3$: a promising Birefringent Crystal. *Inorganic chemistry*, *46*(13), 5207-5211.

Xu, B., Li, T., Zhang, Y., Zhang, Z., Liu, X., & Zhao, J. (2008). New synthetic route and characterization of magnesium borate nanorods. *Crystal Growth and Design*, *8*(4), 1218-1222.

Zhang, G., Wu, Y., Fu, P., Wang, G., Liu, H., Fan, G., & Chen, C. (2002). A new sodium samarium borate $Na_3Sm_2(BO_3)_3$. *Journal of Physics and Chemistry of Solids*, *63*(1), 145-149.